Collisionless modes of a trapped Bose gas

M. J. Bijlsma and H. T. C. Stoof
Institute for Theoretical Physics, University of Utrecht, Princetonplein 5, 3584 CC Utrecht, The Netherlands
(Received 4 February 1999)

We calculate the excitation frequencies of low-lying modes of a trapped Bose-condensed gas at nonzero temperatures. In our calculation we include the dynamics of the noncondensed cloud, and find agreement with experimental results if we assume that in the experiment both the in-phase and out-of-phase monopole modes are excited simultaneously. In order to explore whether this is indeed the correct explanation, we also calculate how strongly the modes couple to a perturbation of the external trapping potential. [S1050-2947(99)05610-3]

PACS number(s): 03.75.Fi, 67.40.−w, 32.80.Pj, 42.50.Vk

I. INTRODUCTION

Since the experimental realization of Bose-Einstein condensation in magnetically trapped ^{87}Rb, ^{7}Li, and ^{23}Na [1–3] gases, various properties of these Bose-condensed systems have been studied both experimentally and theoretically. A challenging problem that has attracted much attention, but is still only partially resolved, is the temperature dependence of the excitation frequencies of the collective modes of a harmonically confined Bose-condensed gas. In principle, its solution requires solving the coupled dynamics of the condensed and noncondensed parts of a highly inhomogeneous interacting gas [4].

In general, the dynamics of an interacting many-body system can be classified as being either in the hydrodynamic limit or the collisionless limit, and the nature of the collective excitations of the system changes as one goes from one limit to the other [5]. In the hydrodynamic regime the mean free path of the quasiparticles is small relative to the wavelength of the collective excitations. Therefore, one can assume the system to be in local equilibrium. In the case of a Bose-condensed gas, this important assumption leads to a description of the coupled dynamics of the condensate and the noncondensate clouds by the well-known Landau two-fluid equations. The solutions to these equations have been studied by several authors [6–8], and experimentally one is also trying to probe this regime [9]. In contrast, in the collisionless regime there is no local equilibrium because the mean free path of the quasiparticles is much larger than the wavelength of the collective modes. Up to now, most experiments with Bose-condensed gases have been performed in this regime. What is of prime interest at present is that these experiments, performed in an axially symmetric trapping potential, indicate a strong temperature dependence of the excitation frequencies for temperatures relatively close to the critical temperature T_c [10]. The first attempts to explain this temperature dependence theoretically were unsatisfactory for a number of reasons.

Far below the critical temperature, the collisionless modes of a trapped Bose gas are accurately described by the Gross-Pitaevskii equation. This equation is a nonlinear Schrödinger equation that describes the time evolution of the condensate wave function at temperatures where the noncondensate density is negligible. It is nonlinear because it includes the mean-field interaction of the condensate with itself. Theoretical calculations solving this equation [11–19] are in good agreement with measurements of the low-lying excitation frequencies in this temperature regime [20,21].

However, at higher temperatures the noncondensate fraction becomes large. Therefore, one has to include into the nonlinear Schrödinger equation the effect of the mean-field interaction of the thermal cloud with the condensate. The low-lying excitation frequencies predicted by the resulting nonlinear Schrödinger equation have been found numerically, and show almost no temperature dependence [22,23]. The lack of temperature dependence can partly be cured by including in the effective two-particle interaction the many-body effects of the surrounding gas on the collisions. This causes the interaction to become strongly temperature dependent [24] and the frequencies of the low-lying modes then also depend on temperature [25]. The frequency of the mode with the azimuthal quantum number $m=2$ found in this way agrees with experiments quite well. This is, however, not the case for the $m=0$ mode.

The latter is related to a fundamental problem with the nonlinear Schrödinger equation used, which describes the dynamics of the condensate in the presence of a static noncondensed cloud. As a result it violates the generalized Kohn theorem, which states that for a harmonically confined many-particle system there are exactly three center-of-mass modes with excitation frequencies equal to the three trapping frequencies. Clearly, this is caused by the fact that we also have to describe the time evolution of the thermal cloud. Therefore, we proposed to describe the collective excitations in the collisionless regime by a nonlinear Schrödinger equation for the condensate wave function, which is coupled to a collisionless Boltzmann or Vlasov-Landau equation, describing the dynamics of the noncondensed cloud [26,27]. The resulting theory contains the Kohn modes exactly.

In our view, therefore, the consistent treatment of the coupled dynamics of the condensed and noncondensed clouds implies that the low-lying collective modes cannot be described solely by the Bogoliubov–de Gennes equations for the wave functions $u(\mathbf{x},t)$ and $v(\mathbf{x},t)$, since these determine only the dynamics of the condensate cloud. In addition we need a dynamical equation for the noncondensate part of the gas. For the experimental conditions of interest, this dynamical equation will take the form of a collisionless Boltzmann equation. Note that such an equation can indeed describe the collective motion of the noncondensed particles, in an analo-

gous way to the treatment of zero sound in liquid ^{3}He [28]. In the latter case, zero sound is a result of slight changes in the occupation numbers of the one-particle states near the Fermi surface. In a Bose gas, however, the collective dynamics will be determined primarily by the one-particle states with thermal energies.

Even above the critical temperature, solving the collisionless Boltzmann equation for the collective modes of the gas is not straightforward. As an illustration, we note that this equation also contains hydrodynamic modes as a special class of solutions. However, we are particularly interested in temperatures relatively close to the critical temperature, where the discrepancy between theory and experiment is largest. Therefore, we want to formulate a manageable theory that has the correct behavior both near zero temperature and near the critical temperature. With this objective in mind, we can treat the thermal cloud in the Hartree-Fock approximation, because near the critical temperature the mean-field interaction is small compared to the average kinetic energy of the noncondensed atoms. Moreover, near zero temperature the presence of the thermal cloud is unimportant.

Finally, to solve the resulting set of coupled partial differential equations that describe the dynamics of the trapped Bose-condensed gas in the time-dependent Hartree-Fock approximation, we apply a dynamical scaling of the ideal gas results for both the condensate wave function and the Wigner distribution describing the noncondensed cloud. This is motivated by the fact that the experiments of interest excite only modes in which both the condensed and noncondensed parts of the gas participate in breathing like oscillations, which can indeed be expected to be captured by a dynamical scaling ansatz.

The paper is organized as follows. In Sec. II we present the general theoretical framework that describes collisionless dynamics of a trapped Bose-condensed gas. In Sec. III we show how the excitation frequencies of the low-lying modes can be determined by means of a dynamical scaling ansatz. We give a physical motivation for our ansatz, and argue in particular that it is accurate near the critical temperature. In Sec. IV we show how the linear response to an external perturbation of the trapping frequency is calculated in our approach. This calculation is performed for reasons that become clear later on in Sec. V, when we compare our results with the experiment. We end the paper in Sec. VI with a summary of our conclusions and an outlook.

II. COLLISIONLESS DYNAMICS

In the Heisenberg picture, the quantum-mechanical evolution of a many-body system of Bose particles in an external trapping potential can be described by a field operator $\hat{\psi}(\mathbf{x},t)$ and a Hamiltonian

$$\hat{H}=\int d\mathbf{x}\Bigg[\hat{\psi}^\dagger(\mathbf{x},t)\mathcal{H}_0\hat{\psi}(\mathbf{x},t)+\frac{1}{2}\int d\mathbf{x}'\hat{\psi}^\dagger(\mathbf{x},t)\hat{\psi}^\dagger(\mathbf{x}',t)V(\mathbf{x}-\mathbf{x}')\hat{\psi}(\mathbf{x}',t)\hat{\psi}(\mathbf{x},t)\Bigg], \tag{1}$$

where $V(\mathbf{x}-\mathbf{x}')$ is the two particle interaction, the single-particle Hamiltonian $\mathcal{H}_0$ is given by

$$\mathcal{H}_0=-\frac{\hbar^2\nabla^2}{2m}+V_{\rm ext}(\mathbf{x}), \tag{2}$$

and $V_{\rm ext}(\mathbf{x})=\Sigma_i m\omega_i^2 x_i^2/2$ denotes the external trapping potential. The field operator satisfies the equal-time commutation relations

$$[\hat{\psi}(\mathbf{x},t),\hat{\psi}(\mathbf{x}',t)]=0,\qquad [\hat{\psi}(\mathbf{x},t),\hat{\psi}^\dagger(\mathbf{x}',t)]=\delta(\mathbf{x}-\mathbf{x}'). \tag{3}$$

By definition, the time evolution of the field operators is determined by the Heisenberg equation of motion

$$i\hbar\frac{\partial\hat{\psi}(\mathbf{x},t)}{\partial t}=[\hat{\psi}(\mathbf{x},t),\hat{H}]. \tag{4}$$

From this equation we can now easily derive an equation of motion for the condensate wave function $\Psi(\mathbf{x},t)$, which is defined as the expectation value $\langle\hat{\psi}(\mathbf{x},t)\rangle$. Applying a mean-field approximation results in a nonlinear Schrödinger equation for $\Psi(\mathbf{x},t)$, which includes the mean-field interaction with the noncondensate density $n'(\mathbf{x},t)$. It reads

$$i\hbar\frac{\partial\Psi(\mathbf{x},t)}{\partial t}=\Bigg\{-\frac{\hbar^2\nabla^2}{2m}+V_{\rm ext}(\mathbf{x})+T^{2B}[2n'(\mathbf{x},t)+n_0(\mathbf{x},t)]\Bigg\}\Psi(\mathbf{x},t). \tag{5}$$

Here the condensate density $n_0(\mathbf{x},t)$ is defined as the modulus squared of the condensate wave function, i.e., $|\Psi(\mathbf{x},t)|^2$. The factor of two difference between the condensate and noncondensate mean-field interactions is understood physically by realizing that the noncondensate contributes both a Hartree term and a Fock term, but the condensate only a Hartree term. Furthermore, the two-body interaction has been renormalized to a hard-core potential $T^{2B}\delta(\mathbf{x}-\mathbf{x}')$, where the two-body scattering matrix $T^{2B}=4\pi\hbar^2 a/m$ solves the Lippmann-Schwinger equation for the scattering of two particles with zero momentum, and a denotes the interatomic scattering length. In principle, the anomalous average has renormalized the two-body interaction potential to the many-body T matrix $T^{\rm MB}$, which also includes the effect of the surrounding gas on the collisions between two particles [29]. For simplicity, however, we will use the two-body scattering matrix instead, neglecting the effective temperature dependence of the two-body interactions. We will briefly comment on the effects of using the many-body T matrix on our results at the end of the paper.

Next we want to derive an equation of motion for the noncondensed cloud. This is achieved by considering the Heisenberg equation of motion for the one-particle density matrix,

$$G(\mathbf{x},\mathbf{x}',t)\equiv\begin{pmatrix}\langle\hat{\psi}'^\dagger(\mathbf{x},t)\hat{\psi}'(\mathbf{x}',t)\rangle & \langle\hat{\psi}'(\mathbf{x},t)\hat{\psi}'(\mathbf{x}',t)\rangle\\ \langle\hat{\psi}'^\dagger(\mathbf{x},t)\hat{\psi}'^\dagger(\mathbf{x}',t)\rangle & \langle\hat{\psi}'(\mathbf{x},t)\hat{\psi}'^\dagger(\mathbf{x}',t)\rangle\end{pmatrix}. \tag{6}$$

Here the field operator describing the noncondensate is defined according to $\hat{\psi}'(\mathbf{x},t)\equiv\hat{\psi}(\mathbf{x},t)-\Psi(\mathbf{x},t)$. From the resulting equation of motion, we can derive a Boltzmann equation describing the time evolution of the quasiparticle distribution function in the usual fashion, which is summarized as follows [5,27].

First, we write the equations of motion for the one-particle density matrix in terms of the relative and center-of-mass coordinates, i.e., $\mathbf{r}\equiv(\mathbf{x}-\mathbf{x}')$ and $\mathbf{R}\equiv(\mathbf{x}+\mathbf{x}')/2$, respectively, and perform a gradient expansion up to first order in $\nabla_{\mathbf{R}}$. This is justified because in general the noncondensate density profile varies on a much larger length scale than the external trapping potential. In the Popov approximation [30] the resulting equation reads

$$i\hbar\frac{\partial G}{\partial t} = \begin{pmatrix} -\frac{\hbar^2}{2m}\nabla_{\mathbf{r}}\cdot\nabla_{\mathbf{R}}+\mathbf{r}\cdot\nabla_{\mathbf{R}}[V_{\rm ext}+\hbar\Sigma_{11}] & \mathbf{r}\cdot\nabla_{\mathbf{R}}\hbar\Sigma_{12} \\ \mathbf{r}\cdot\nabla_{\mathbf{R}}\hbar\Sigma_{21} & -\frac{\hbar^2}{2m}\nabla_{\mathbf{r}}\cdot\nabla_{\mathbf{R}}+\mathbf{r}\cdot\nabla_{\mathbf{R}}[V_{\rm ext}+\hbar\Sigma_{22}] \end{pmatrix} G, \tag{7}$$

where the diagonal self-energies are $\hbar\Sigma_{11}(\mathbf{R},t)=\hbar\Sigma_{22}(\mathbf{R},t)=2T^{2B}[n'(\mathbf{R},t)+n_0(\mathbf{R},t)]$, and the off-diagonal or anomalous self-energies are $\hbar\Sigma_{12}(\mathbf{R},t)=T^{2B}[\Psi(\mathbf{R},t)]^2$ and $\hbar\Sigma_{21}(\mathbf{R},t)=T^{2B}[\Psi^*(\mathbf{R},t)]^2$. Second, we Fourier transform Eq. (7) with respect to $\mathbf{r}$. Finally, the one-particle density matrix $G(\mathbf{k},\mathbf{R},t)$ is then diagonalized by means of a local Bogoliubov transformation. The final equations for the nonvanishing elements $G_{11}(\mathbf{k},\mathbf{R},t)=F(\mathbf{k},\mathbf{R},t)$ and $G_{22}(\mathbf{k},\mathbf{R},t)=1+F(\mathbf{k},\mathbf{R},t)$, where $F(\mathbf{k},\mathbf{R},t)$ is by definition the quasiparticle distribution function, turn out to be identical, and lead to the desired Boltzmann equation for the noncondensate distribution function, which from now on we again denote by $F(\mathbf{k},\mathbf{x},t)$.

This Boltzmann equation contains two streaming terms, corresponding to the local group velocity of a quasiparticle and the local force on a quasiparticle. The velocity and the force are given by the momentum and the spatial derivative of the energy dispersion $E(\mathbf{k},\mathbf{x},t)$, respectively. The distribution of quasiparticles can also change because of collisions and on the right-hand side there is an associated collision term. In total the Boltzmann equation therefore reads

$$\left[\frac{\partial}{\partial t}+\frac{\partial E}{\partial\hbar\mathbf{k}}\cdot\frac{\partial}{\partial\mathbf{x}}-\frac{\partial E}{\partial\mathbf{x}}\cdot\frac{\partial}{\partial\hbar\mathbf{k}}\right]F=\left[\frac{\partial F}{\partial t}\right]_{\rm coll.}. \tag{8}$$

If we treat the quasiparticles in the Popov approximation, their energy, in the frame where the superfluid velocity $v_s(\mathbf{x},t)$ is zero, is given by

$$E(\mathbf{x},\mathbf{k},t)=\left(\left[\frac{\hbar^2\mathbf{k}^2}{2m}+V_{\rm ext}(\mathbf{x})+2T^{2B}n(\mathbf{x},t)+\hbar\dot{\theta}(\mathbf{x},t)+\frac{mv_s^2(\mathbf{x},t)}{2}\right]^2-[T^{2B}n_0(\mathbf{x},t)]^2\right)^{1/2}+\hbar\mathbf{k}\cdot\mathbf{v}_s(\mathbf{x},t). \tag{9}$$

Here $\theta(\mathbf{x},t)$ is the phase of the condensate wave function, i.e., $\Psi(\mathbf{x},t)=\sqrt{n_0(\mathbf{x},t)}\exp i\theta(\mathbf{x},t)$. Furthermore, the superfluid velocity is proportional to the gradient of that phase, or more precisely $\mathbf{v}_s(\mathbf{x},t)=\hbar\nabla\theta(\mathbf{x},t)/m$.

In the temperature region of interest it is sufficient to treat the quasiparticles in the Hartree-Fock approximation. The energy in the laboratory frame is then given by

$$E(\mathbf{x},\mathbf{k},t)=\frac{\hbar^2\mathbf{k}^2}{2m}+V_{\rm ext}(\mathbf{x})+2T^{2B}n(\mathbf{x},t). \tag{10}$$

The resulting nonlinear Schrödinger equation and collisionless Boltzmann equation are expected to describe the dynamics of the trapped Bose gas near the critical temperature T_c, because in this temperature region the mean-field interaction of the condensate is small compared to the average kinetic energy of the noncondensed cloud, implying that the Hartree-Fock approximation is valid. Moreover, they will also be accurate near zero temperature, because here the noncondensate density is negligible.

III. VARIATIONAL APPROACH

Directly solving the set of equations that describe the coupled collisionless dynamics of the condensate and the noncondensate, i.e., the nonlinear Schrödinger equation given by Eq. (5) and the collisionless Boltzmann equation following from Eq. (8), is difficult even when treating the quasiparticles in the Hartree-Fock approximation. However, it is well known that a simple scaling ansatz for the condensate wave function gives the correct frequencies of the low-lying modes at zero temperature [14,15]. Therefore, we use a similar method to solve our set of equations, and also assume the time dependence of the quasiparticle distribution function to be given by a dynamical scaling ansatz. We thus obtain

$$n_0(\mathbf{x},t)=\left[\prod_j\frac{1}{\lambda_j}\right]\Phi_{n_0}\left(\left\{\frac{x_i-\eta_i^{(1)}}{\lambda_i}\right\}\right), \tag{11a}$$

$$\theta(\mathbf{x},t)=\sum_i\frac{m\omega_i}{\hbar}[\eta_i^{(3)}x_i+\beta_i x_i^2], \tag{11b}$$

$$F(\mathbf{k},\mathbf{x},t)=\left[\prod_j c_j\right]\Phi_F\left(\left\{\sqrt{c_i}\left[\frac{x_i-\eta_i^{(2)}}{\alpha_i}\right]\right\},\left\{\sqrt{c_i}\alpha_i\left[k_i-\frac{m}{\hbar}\frac{\dot{\alpha}_i}{\alpha_i}[x_i-\eta_i^{(2)}]-\frac{m}{\hbar}\dot{\eta}_i^{(2)}\right]\right\}\right). \tag{11c}$$

Here Φ_{n_0} and Φ_F are still arbitrary functions, but their precise form will be motivated below. The six parameters $\{\lambda_i\}$ and $\{\alpha_i\}$ describe the coupled monopole and quadrupole oscillations of the two components of the gas. The six parameters $\{\eta_i^{(1)}\}$ and $\{\eta_i^{(2)}\}$ are included to describe the in-phase and out-of-phase dipole, or Kohn, modes. Notice that the momentum argument of the scaling ansatz for the distribution function contains explicit time derivatives of the scaling parameters. Together with the quadratic form of the phase, this ensures that the continuity equation is satisfied. The variational parameters $\{\eta_i^{(3)}\}$ and $\{\beta_i\}$ are therefore related

to $\{\eta_i^{(1)}\}$ and $\{\lambda_i\}$ in a way specified below. Due to the mean-field interaction, the equilibrium values of $\{\lambda_i\}$ and $\{\alpha_i\}$ are in general not equal to 1. In order to ensure that the equilibrium profile is isotropic in momentum space, the factors $\{c_i\}$ are inserted, which are equal to $1/\overline{\alpha_i^2}$, where $\overline{\alpha_i}$ denotes the equilibrium value of α_i. The modes of the noncondensed cloud described by this ansatz, are, however, not constrained to be isotropic in momentum space. Hence they describe more complicated dynamics than hydrodynamic motion, as desired in the collisionless limit.

The equations of motion for the scaling parameters of the condensate are most easily found from the Lagrangian density for the nonlinear Schrödinger equation written in terms of the density and the phase:

$$\mathcal{L}=\hbar n_0(\mathbf{x},t)\frac{\partial\theta(\mathbf{x},t)}{\partial t}+\frac{\hbar^2}{2m}\frac{[\nabla n_0(\mathbf{x},t)]^2}{4n_0(\mathbf{x},t)}+\frac{\hbar^2}{2m}n_0(\mathbf{x},t)[\nabla\theta(\mathbf{x},t)]^2+\left[V_{\rm ext}(\mathbf{x})+2T^{2B}n'(\mathbf{x},t)+\frac{T^{2B}}{2}n_0(\mathbf{x},t)\right]n_0(\mathbf{x},t). \tag{12}$$

Inserting the scaling ansatz for the density and the appropriate phase into this Lagrangian density, and integrating over space, yields a Lagrangian for the scaling parameters. The equations of motion for these parameters are then given by the appropriate Euler-Lagrange equations. The equations of motion for the scaling parameters of the noncondensate are found by taking moments of the collisionless Boltzmann equation with respect to k_i, x_i, k_ik_j, x_ik_i, and x_ix_j.

The resulting equations of motion for the in total 12 variational parameters are

$$\ddot{\eta}_i^{(1)}+\omega_i^2\eta_i^{(1)}=-\frac{2T^{2B}}{mN_0}\frac{\partial}{\partial\eta_i^{(1)}}\langle\Phi_{n'}(\boldsymbol{\xi}_1)\rangle_c\prod_j\frac{\sqrt{c_j}}{\alpha_j}, \tag{13a}$$

$$\ddot{\eta}_i^{(2)}+\omega_i^2\eta_i^{(2)}=-\frac{2T^{2B}}{mN'}\frac{\partial}{\partial\eta_i^{(2)}}\langle\Phi_{n_0}(\boldsymbol{\xi}_2)\rangle_{nc}\prod_j\frac{1}{\lambda_j}, \tag{13b}$$

$$\ddot{\lambda}_i+\omega_i^2\lambda_i=\frac{T_i^{\rm kin,c}}{m\langle x_i^2\rangle_c}\frac{2}{\lambda_i^3}+\frac{T^{2B}\langle\Phi_{n_0}(\mathbf{x})\rangle_c}{2m\langle x_i^2\rangle_c}\frac{1}{\lambda_i}\prod_j\frac{1}{\lambda_j}-\frac{2T^{2B}}{m\langle x_i^2\rangle_c}\frac{\partial}{\partial\lambda_i}\langle\Phi_{n'}(\boldsymbol{\xi}_1)\rangle_c\prod_j\frac{\sqrt{c_j}}{\alpha_j}, \tag{13c}$$

$$\ddot{\alpha}_i+\omega_i^2\alpha_i=\frac{T_i^{\rm kin,nc}}{m\langle x_i^2\rangle_{nc}}\frac{2}{\alpha_i^3}+\frac{T^{2B}\langle\Phi_{n'}(\mathbf{x})\rangle_{nc}}{m\langle x_i^2\rangle_{nc}}\frac{c_i}{\alpha_i}\prod_j\frac{\sqrt{c_j}}{\alpha_j}-\frac{2T^{2B}}{m\langle x_i^2\rangle_{nc}}\frac{\partial}{\partial\alpha_i}\langle\Phi_{n_0}(\boldsymbol{\xi}_2)\rangle_{nc}\prod_j\frac{1}{\lambda_j}, \tag{13d}$$

whereas the dynamics of the phase is determined by

$$\beta_i=\frac{1}{2\omega_i}\frac{\dot{\lambda}_i}{\lambda_i}, \tag{14a}$$

$$\eta_i^{(3)}=-2\beta_i\eta_i^{(1)}+\frac{\dot{\eta}_i^{(1)}}{\omega_i}. \tag{14b}$$

For notational convenience we have defined the arguments $\boldsymbol{\xi}_1$ and $\boldsymbol{\xi}_2$ by

$$\xi_{1,i}=(\lambda_ix_i+\eta_i^{(1)}-\eta_i^{(2)})\sqrt{c_i}/\alpha_i, \tag{15a}$$

$$\xi_{2,i}=(\alpha_ix_i/\sqrt{c_i}+\eta_i^{(2)}-\eta_i^{(1)})/\lambda_i. \tag{15b}$$

Also, the kinetic energy of the condensate and noncondensate are given by

$$T_i^{\rm kin,c}=\int d\mathbf{x}\frac{\hbar^2}{2m}\frac{[\partial_i\Phi_{n_0}(\mathbf{x})]^2}{4\Phi_{n_0}(\mathbf{x})} \tag{16}$$

and

$$T_i^{\rm kin,nc}=\int d\mathbf{x}\int\frac{d\mathbf{k}}{(2\pi)^3}\frac{\hbar^2k_i^2}{2m}\Phi_F(\mathbf{x},\mathbf{k}), \tag{17}$$

respectively. Finally, the weighted averages with respect to the equilibrium condensate and noncondensate densities are

$$\langle f(\mathbf{x})\rangle_c=\int d\mathbf{x}\Phi_{n_0}(\mathbf{x})f(\mathbf{x}) \tag{18}$$

and

$$\langle f(\mathbf{x})\rangle_{nc}=\int d\mathbf{x}\Phi_{n'}(\mathbf{x})f(\mathbf{x}), \tag{19}$$

where $\Phi_{n'}(\mathbf{x})=(2\pi)^{-3}\int d\mathbf{k}\,\Phi_F(\mathbf{x},\mathbf{k})$. Note that the equations of motion for $\{\lambda_i\}$ and $\{\alpha_i\}$ are of the same form, apart from a factor of 2 difference between the mean-field interaction of the condensate with itself and the mean-field interaction of the noncondensate with itself. Of course, this is the same factor of 2 difference that was mentioned above in relation to the nonlinear Schrödinger equation.

In the Thomas-Fermi limit we can neglect the average kinetic energy of the condensate relative to the mean-field interactions, and the ground-state density profile of the condensate is approximately an inverted parabola. The opposite limit, where the mean-field interaction is much less than the average kinetic energy, results in a Gaussian density profile. For the experiments of interest here, a Gaussian profile is appropriate near the critical temperature. At low temperatures this is no longer true, and an inverted parabola is more accurate. However, for our purposes it is convenient to take at all temperatures a Gaussian ansatz for the condensate, because it is known to give the correct frequencies even at zero temperature [15]. Hence

$$\Phi_{n_0}(\mathbf{x})=N_0\prod_j\left(\frac{m\omega_j}{\hbar\pi}\right)^{1/2}e^{-\sum_i(m\omega_i/\hbar)x_i^2}. \tag{20}$$

Since the effect of the noncondensate is most important near T_c, we take the dynamical scaling ansatz for the quasi-

particle distribution to be a Bose function. Near the critical temperature and neglecting mean-field interactions, this indeed gives the correct mode frequencies, i.e., $\{2\omega_i\}$. We thus take

$$\Phi_F(\mathbf{x},\mathbf{k}) = \frac{N' \prod_j (\beta\hbar\omega_j)}{\zeta(3)} N\left(\frac{\hbar^2 k^2}{2m} + \sum_i \frac{m\omega_i^2 x_i^2}{2} \right), \tag{21}$$

where $N(\varepsilon)$ is the usual Bose distribution function:

$$N(\varepsilon) = [e^{\beta\varepsilon} - 1]^{-1}. \tag{22}$$

Here $\beta = 1/k_B T$ and $\zeta(3) \approx 1.202$. The normalization factors are such that the total numbers of condensed and noncondensed atoms are equal to N_0 and N', respectively. We take the temperature dependence of the total number of condensed atoms to be given by the noninteracting result $N_0 = [1 - (T/T_c)^3]N$, where $N = N_0 + N'$ is the total number of particles. At this point we should note that our scaling ansatz can only describe coupled breathing-type oscillations of both the condensate and noncondensate clouds. This is sufficient for our purposes, since these are the only modes that have up to now been seen experimentally.

The equations of motion for the scaling parameters that result from inserting Eqs. (20) and (21) into Eq. (13) are listed in the Appendix. If we introduce vector notation

$$\mathbf{u}_1 = \begin{pmatrix} \boldsymbol{\lambda} \\ \boldsymbol{\alpha} \end{pmatrix}, \tag{23a}$$

$$\mathbf{u}_2 = \begin{pmatrix} \boldsymbol{\eta}^{(1)} \\ \boldsymbol{\eta}^{(2)} \end{pmatrix}, \tag{23b}$$

$$\boldsymbol{\Omega} = \begin{pmatrix} \boldsymbol{\omega} & 0 \\ 0 & \boldsymbol{\omega} \end{pmatrix}, \tag{23c}$$

where $\boldsymbol{\omega}_{ij} = \delta_{ij}\omega_i$, these can be schematically written as

$$\ddot{\mathbf{u}}_1 + \boldsymbol{\Omega}^2 \cdot \mathbf{u}_1 = \mathbf{v}(\mathbf{u}_1, \mathbf{u}_2), \tag{24a}$$

$$\ddot{\mathbf{u}}_2 + \boldsymbol{\Omega}^2 \cdot \mathbf{u}_2 = \mathbf{w}(\mathbf{u}_1, \mathbf{u}_2), \tag{24b}$$

with $\mathbf{v}$ and $\mathbf{w}$ nonlinear vector functions of their arguments. To find the excitation frequencies of the modes, we have to linearize these equations around the equilibrium value $(\overline{\mathbf{u}_1}, \overline{\mathbf{u}_2})$, and subsequently determine the eigenvectors and eigenvalues of the linearized problem. From the explicit expressions in the Appendix, it is easily seen that the linearized equations for $\delta\mathbf{u}_1$ and $\delta\mathbf{u}_2$ decouple. The resulting excitation frequencies for the in-phase and out-of-phase monopole, quadrupole, and dipole, or Kohn, modes are presented and discussed in Sec. V below.

IV. LINEAR RESPONSE

In order to compare our theoretical results with experiment, it turns out to be important to understand what is measured experimentally when the external trapping potential is perturbed to excite the collective modes of the Bose-condensed gas. It is possible that a periodic modulation of the trapping frequency will excite more than one mode when it is not exactly on resonance. The question is then which mode is most likely to be seen experimentally. To answer this question we have to study the linearized response of the gas to a periodic perturbation of the trapping frequencies

$$\omega_i \to \omega_i + \delta\omega_i e^{i\omega t}, \tag{25}$$

leading to

$$V_{\text{ext}}(\mathbf{x}) \to V_{\text{ext}}(\mathbf{x}) + \delta V_{\text{ext}}(\mathbf{x}) e^{i\omega t} \tag{26}$$

and

$$n(\mathbf{x},t) \to n(\mathbf{x}) + \delta n(\mathbf{x}) e^{i\omega t}. \tag{27}$$

A quantity that characterizes the response to such a perturbation is the time-averaged work done by the perturbation [31],

$$W = \frac{1}{2} \int d\mathbf{x} \delta V_{\text{ext}}(\mathbf{x}) \delta n^*(\mathbf{x}), \tag{28}$$

where the asterisk denotes the complex conjugate. An explicit expression for the time-averaged work is found by linearizing the density profiles around equilibrium, by putting $\lambda_i = \overline{\lambda}_i + \delta\lambda_i e^{i\omega t}$ and $\alpha_i = \overline{\alpha}_i + \delta\alpha_i e^{i\omega t}$. If we insert the resulting expression for $\delta n = \delta n_0 + \delta n'$ into Eq. (28), we obtain

$$W = \sum_i m\omega_i \delta\omega_i [\overline{\lambda}_i \delta\lambda_i^* \langle x_i^2 \rangle_c + \overline{\alpha}_i \delta\alpha_i^* \langle x_i^2 \rangle_{nc}]. \tag{29}$$

To calculate the work done by the perturbation, we thus need to know the response of the scaling parameters to a perturbation of the external potential.

After linearizing the equations of motion Eq. (24a), with $\mathbf{u}_2 = 0$, to first order in $\delta\omega_i$ and $\delta\mathbf{u}_1$, the resulting equation of motion for the fluctuation $\delta\mathbf{u}_1$, reads

$$-\omega^2 \delta\mathbf{u}_1 + \boldsymbol{\Omega}^2 \cdot \delta\mathbf{u}_1 = [\nabla_{u_1} \mathbf{v}] \cdot \delta\mathbf{u}_1 - 2\boldsymbol{\Omega} \cdot \delta\boldsymbol{\Omega} \cdot \overline{\mathbf{u}}_1. \tag{30}$$

The partial derivative of $\mathbf{v}$ with respect to $\mathbf{u}_1$ is to be evaluated in the equilibrium point. These linearized equations of motion are easily solved by

$$\delta\mathbf{u}_1 = \sum_n \frac{a_n}{\omega^2 - \omega_n^2} \mathbf{u}_1^{(n)}, \tag{31}$$

where $\mathbf{u}_1^{(n)}$ denote the normalized eigenvectors of the homogeneous part of Eq. (30), and $a_n = 2\mathbf{u}_1^{(n)} \cdot \boldsymbol{\Omega} \cdot \delta\boldsymbol{\Omega} \cdot \overline{\mathbf{u}}_1$. The time-averaged work done can now be expressed as

$$W = \sum_n \frac{b_n}{\omega^2 - \omega_n^2}, \tag{32}$$

where the residue b_n is given by

$$b_n = \sum_i m\omega_i \delta\omega_i a_n [\overline{\lambda}_i \lambda_i^{(n)} \langle x_i^2 \rangle_c + \overline{\alpha}_i \alpha_i^{(n)} \langle x_i^2 \rangle_{nc}]. \tag{33}$$

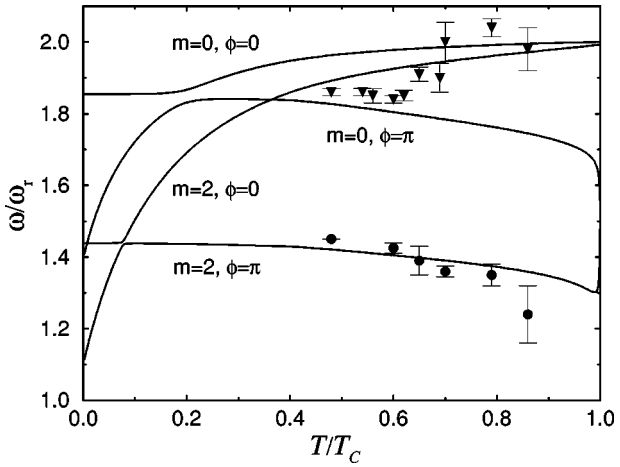

FIG. 1. The in-phase and out-of-phase $m=0$ and 2 modes as a function of T/T_c for the experimental conditions of Jin *et al.* [10]. The relative phase of the density profiles of the condensed and noncondensed atoms is denoted by ϕ. Also included are the experimental results for the $m=0$ (triangles) and $m=2$ (circles) modes found in these experiments.

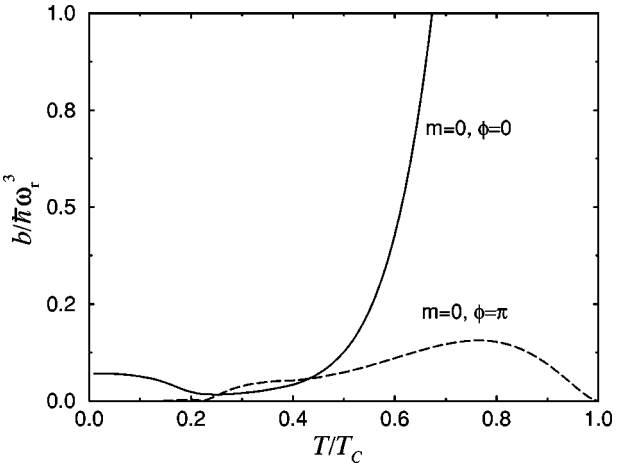

FIG. 2. The residue b for the modes $m=0,\phi=0$ (solid line), and $m=0,\phi=\pi$ (dotted line) as a function of T/T_c for the experimental conditions of Jin *et al.* [10].

In reality, the eigenmodes are damped. Therefore, in a theory that includes damping, the poles ω_n have an imaginary part, and W is always finite with a maximum at $\omega=\omega_n$. Hence a resonance would occur if the system were driven with that frequency. A measure of the strength with which this mode is excited is the residue b_n. Also, the time-averaged work would acquire an imaginary part, which would determine the power absorption. We have calculated the residue b for two particular modes as a function of temperature, and the results are presented in Sec. V.

V. RESULTS

In this section we present the results of our calculations, and if possible compare them with experimental data. In principle our approach determines 12 modes of the gas. In an axially symmetric situation, they correspond to the in-phase and out-of-phase versions of three Kohn modes, two monopole modes, and one quadrupole mode. These in-phase and out-of-phase modes are the collisionless analog of the hydrodynamic first and second sound modes [6–8]. We have calculated the excitation frequencies of these modes for the parameters of the experiments with ^{87}Rb [10], ^{23}Na [9], and ^{7}Li [2]. Furthermore, for the experiments with ^{87}Rb, we have calculated the residue b mentioned in Sec. IV for the in-phase and out-of-phase monopole modes.

From the results presented in Fig. 1, it is clear that the temperature dependence of the out-of-phase $m=2$ mode is in reasonable agreement with that of the $m=2$ mode of the ^{87}Rb experiments. Furthermore, the experimental data for the $m=0$ mode goes to the correct noninteracting limit near T_c, where it coincides with our theoretical curve for the in-phase $m=0$ mode. In addition, between $0.7T_c$ and $0.6T_c$, the experimental data drop to the zero-temperature limit $(10/3)^{1/2}\omega_r$ [11], where they coincide with our theoretical curve for the out-of-phase $m=0$ mode. It is important to note that in obtaining these results, we have included the effect of evaporative cooling by fitting the total number of particles to the experimental results of Jin *et al.* [10]. Qualitatively, it appears that the strong temperature dependence found experimentally might be due to the fact that one simultaneously excites both the in-phase and out-of-phase $m=0$ modes [32]. To explore this possibility we have calculated the residue b for these two modes. As shown in Fig. 2, there is a clear crossover at about $0.5T_c$, after which the value for the residue of the in-phase $m=0$ mode shoots up. Therefore, the experimental data might actually be due to the excitation of two modes, and as a function of temperature one crosses over from exciting mainly one mode to exciting mainly the other. Furthermore, Fig. 2 shows that the out-of-phase $m=0$ mode cannot be seen experimentally below $0.2T_c$, because here the mode is very difficult to excite. Finally, we note that it might be possible to observe the two additional modes present in our calculation experimentally. Whether this is possible depends on the overlap of these modes with the applied perturbation, and on the damping of the modes, which we have neglected.

As mentioned above, our theory reproduces the correct excitation frequencies near the critical temperature and near zero temperature. In principle, sufficiently far below the critical temperature there is a ''dimple'' in the noncondensate density profile due to the presence of a condensate. This dimple is not taken into account in our dynamical scaling ansatz. However, it is incorrect to include this dimple by simply modifying the scaling profile, because we are using a one parameter scaling ansatz. Consider, for example, an out-of-phase mode of the condensate and the noncondensate. Because the dimple is caused by the mean-field interaction with the condensate, it also has to move out of phase with the exterior part of the noncondensed cloud. This implies that there are two length scales that determine the dynamics of the noncondensate. Hence modifying the scaling profile Φ_F, for example, by taking the exact equilibrium solution for the noncondensate density, can actually give worse results. Moreover, neglecting the dimple in the density profile of the noncondensed cloud is certainly correct near the critical temperature. A qualitative reason why the theory still seems to agree well with experiment is that a dimple in the noncondensate density, on the one hand, increases the effective

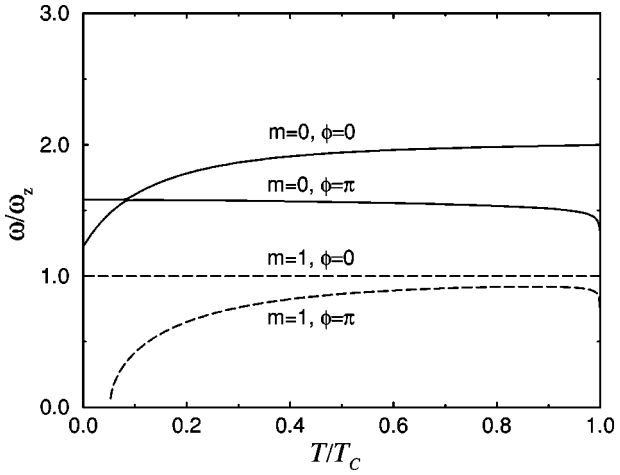

FIG. 3. The in-phase and out-of-phase $m=0$ (solid lines), and Kohn (dashed lines) modes as a function of T/T_c for the experimental conditions of Stamper-Kurn *et al.* [9], with a total number of particles $N=40\times10^6$.

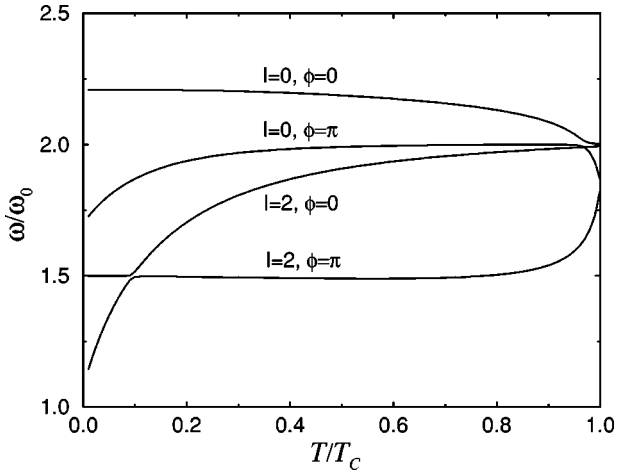

FIG. 4. The in-phase and out-of-phase $l=0$ and 2 modes as a function of T/T_c for an isotropic trap $\omega_x=\omega_y=\omega_z=\omega_0=200$ Hz, and with a total number of atoms $N=2000$.

mass of the condensate, which reduces the excitation frequency, but on the other hand lowers the mean-field interaction, which increases the excitation frequency. Apparently, these two effects almost cancel each other.

In Fig. 3, we show the calculated in-phase and out-of-phase monopole and Kohn modes for the experimental parameters of Stamper-Kurn *et al.* [9]. The Kohn modes are exactly present in our theory, which can be seen by rewriting Eq. (13) in terms of $\eta_i^{(1)}+\eta_i^{(2)}$ and $\eta_i^{(1)}-\eta_i^{(2)}$. The out-of-phase Kohn modes have the qualitatively correct feature found in the experiments, that the frequency of the mode is shifted downward with respect to the trapping frequency. Experimentally the shift is about 5%. Instead, we find a reduction of about 10%. The fact that the out-of-phase dipole mode becomes unstable at $T/T_c\approx0.05$ can be understood by realizing that our equilibrium profile is always centered around the origin. Because we do not include the dimple in the noncondensate density profile, this implies that, at a certain temperature, it is energetically favorable for the noncondensed cloud to shift its center outward. Because the instability occurs only at very low temperatures, this artifact of our ansatz is not of importance for our purposes.

To be able to compare our data with results found in the Popov calculations of Hutchinson *et al.* [22], we have also looked at the case of an isotropic trap. Interestingly, our results, which are shown in Fig. 4, are quite similar to theirs. Moreover, when analyzing the temperature dependence of the mode frequencies by means of a temperature-dependent effective interaction, the results found in the isotropic case are also very similar to these results [33]. This suggests that the interesting temperature dependences are related to the anisotropy of the external trapping potential.

Finally, as shown in Fig. 5, we have also calculated the mode frequencies for the experimental conditions of Bradley *et al.* [2] that apply to the case of a negative scattering length. It should be noted that our approach is particularly suited for a discussion of this case, because the mean-field interaction of the condensate is at most comparable to the energy splitting in the trap, due to the intrinsic instability of the condensate to collapse [34]. As expected, the maximum number of condensate particles is slightly shifted downward by the mean-field interaction of the noncondensate with the condensate. At a temperature of 300 nK, we find a shift of about 3%, whereas more accurate calculations find a shift of about 5% [35]. In addition, the dynamical treatment of the noncondensed cloud seems to have little effect on the mode frequencies. This indicates that it is a good approximation to treat the collapse purely in terms of the condensate even at nonzero temperatures [36].

VI. CONCLUSION AND OUTLOOK

If we interpret the temperature dependence of the $m=0$ mode found in the JILA experiments as due to the excitation of two modes instead of one, there seems to be reasonable agreement between our theoretical predictions and the experimental results. We should mention, however, that our results are sensitive to the explicit form of the ansatz. Indeed, work done by the authors in collaboration with Zaremba shows that using a numerical solution for the condensate and noncondensate equilibium density profiles in the Popov ap-

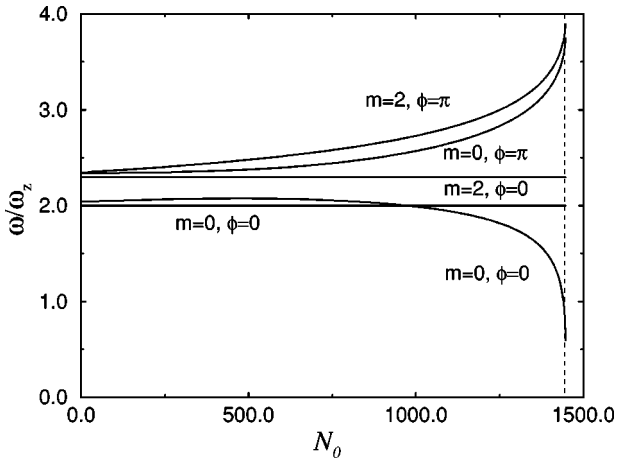

FIG. 5. The in-phase and out-of-phase $m=0$ and 2 modes at a constant temperature $T=300$ nK, as a function of the number of atoms in the condensate, for the experimental conditions of Bradley *et al.* [2]. The condensate collapses for $N_0=1447$.

proximation for the ansatz leads to qualitatively different results. However, as mentioned above, we believe this to be due to the one-parameter nature of the ansatz used. It is a matter of future investigation to resolve this problem, possibly by including more variational parameters into the density profile. Alternatively, we can perform a random-phase-approximation calculation of the mode frequencies [37], which is essentially equivalent to finding the modes of the collisionless Boltzmann equation coupled to the nonlinear Schrödinger equation exactly [5].

In principle we should also take the effect of replacing the two-body T matrix with the many-body T matrix into consideration. As shown in Ref. [25], this will shift the frequencies of the out-of-phase modes downward and presumably improve the agreement of our results with the experimental data. However, we believe that the effect on the modes that are predominantly due to the noncondensate will be negligible because of fact that for collisions of noncondensed particles with thermal energies the many-body T matrix becomes equal to the two-body T matrix. Hence the inclusion of these effects will not alter our conclusion about the temperature dependence of the $m=0$ mode.

Finally, we can in principle also calculate the damping of these modes within our approach, by including the collision terms in the Boltzmann equation [38]. Work to implement these ideas is in progress. After submission of this paper we received a preprint by Guéry-Odelin *et al.* [39], in which the damping of the low-lying modes in a classical Bose gas above the critical temperature was calculated in the way outlined above.

ACKNOWLEDGMENTS

It is a pleasure to thank E. Zaremba for many fruitful discussions and for collaborating in the calculation of the mode frequencies with equilibrium density profiles as our ansatz. Furthermore, we acknowledge illuminating comments by E.A. Cornell, F. Langeveld, and C.J. Pethick.

APPENDIX: EQUATIONS OF MOTION

Here we list the equations of motion for the variational parameters $\{\lambda_i\}$, $\{\alpha_i\}$, $\{\eta_i^{(1)}\}$, and $\{\eta_i^{(2)}\}$ resulting from inserting the explicit form of the condensate wave function and the noncondensate distribution function Eqs. (20) and (21) into Eqs. (13). The average harmonic-oscillator length is defined by $\overline{l}=\sqrt{\hbar/m\overline{\omega}}$, where $\overline{\omega}=(\omega_1\omega_2\omega_3)^{1/3}$. The thermal wavelength is given by $\Lambda_{\rm th}=\sqrt{2\pi\hbar^2/mk_BT}$, and $\zeta(4)\approx 1.082$. Note that in equilibrium $\eta_i^{(1)}=\eta_i^{(2)}=0$ and that the equations for $\{\lambda_i,\alpha_i\}$ and $\{\eta_i^{(1)},\eta_i^{(2)}\}$ decouple when they are linearized around this equilibrium.

$$\frac{\ddot{\eta}_i^{(1)}}{\omega_i^2}+\eta_i^{(1)}=\frac{4\zeta(3)^{-1}}{\pi^3\sqrt{2}}\left(\frac{N'a}{\overline{l}}\right)\left(\frac{\Lambda_{\rm th}}{\overline{l}}\right)^5\sum_{n=1}^{\infty}\frac{1}{n^{1/2}}\prod_j\left[\frac{1}{n\beta\hbar\omega_j\lambda_j^2+2\alpha_j^2\overline{\alpha_j^2}}\right]^{1/2}\frac{\eta_i^{(1)}-\eta_i^{(2)}}{n\beta\hbar\omega_i\lambda_i^2+2\alpha_i^2\overline{\alpha_i^2}}$$
$$\times\exp\left(\sum_i\frac{-n\beta m\omega_i^2[\eta_i^{(1)}-\eta_i^{(2)}]^2}{n\beta\hbar\omega_i\lambda_i^2+2\alpha_i^2\overline{\alpha_i^2}}\right), \tag{A1}$$

$$\frac{\ddot{\eta}_i^{(2)}}{\omega_i^2}+\eta_i^{(2)}=\frac{4\zeta(3)^{-1}}{\pi^3\sqrt{2}}\left(\frac{N_0a}{\overline{l}}\right)\left(\frac{\Lambda_{\rm th}}{\overline{l}}\right)^5\sum_{n=1}^{\infty}\frac{1}{n^{1/2}}\prod_j\left[\frac{1}{n\beta\hbar\omega_j\lambda_j^2+2\alpha_j^2\overline{\alpha_j^2}}\right]^{1/2}\frac{\eta_i^{(2)}-\eta_i^{(1)}}{n\beta\hbar\omega_i\lambda_i^2+2\alpha_i^2\overline{\alpha_i^2}}$$
$$\times\exp\left(\sum_i\frac{-n\beta m\omega_i^2[\eta_i^{(2)}-\eta_i^{(1)}]^2}{n\beta\hbar\omega_i\lambda_i^2+2\alpha_i^2\overline{\alpha_i^2}}\right), \tag{A2}$$

$$\frac{\ddot{\lambda}_i}{\omega_i^2}+\lambda_i=\frac{1}{\lambda_i^3}+\sqrt{\frac{2}{\pi}}\frac{N_0a}{\overline{l}}\left(\frac{l_i}{\overline{l}}\right)^2\prod_j\left[\frac{1}{\lambda_j}\right]\frac{1}{\lambda_i}+\frac{4\zeta(3)^{-1}}{\pi^3\sqrt{2}}\left(\frac{N'a}{\overline{l}}\right)\left(\frac{\Lambda_{\rm th}}{\overline{l}}\right)^5\sum_{n=1}^{\infty}\frac{1}{n^{1/2}}\prod_j\left[\frac{1}{n\beta\hbar\omega_j\lambda_j^2+2\alpha_j^2\overline{\alpha_j^2}}\right]^{1/2}\frac{\lambda_i}{n\beta\hbar\omega_i\lambda_i^2+2\alpha_i^2\overline{\alpha_i^2}}$$
$$\times\left[1+\frac{2n\beta m\omega_i^2[\eta_i^{(1)}-\eta_i^{(2)}]^2}{n\beta\hbar\omega_i\lambda_i^2+\alpha_i^2\overline{\alpha_i^2}}\right]\exp\left(\sum_i\frac{-n\beta m\omega_i^2[\eta_i^{(1)}-\eta_i^{(2)}]^2}{n\beta\hbar\omega_i\lambda_i^2+2\alpha_i^2\overline{\alpha_i^2}}\right), \tag{A3}$$

$$\frac{\ddot{\alpha}_i}{\omega_i^2}+\alpha_i=\frac{1}{\alpha_i^3}+\frac{1}{2\pi^3}\left(\frac{\Lambda_{\rm th}}{\overline{l}}\right)^5\left(\frac{N'a}{\overline{l}}\right)\frac{\left[\sum_{n,m=1}^{\infty}n^{-1/2}m^{-3/2}(n+m)^{-5/2}\right]}{\zeta(3)\zeta(4)}\left[\prod_j\frac{1}{\alpha_j\overline{\alpha_j}}\right]\frac{1}{\alpha_i\overline{\alpha_j^2}}+\frac{4\zeta(4)^{-1}}{\pi^3\sqrt{2}}\left(\frac{N_0a}{\overline{l}}\right)$$
$$\times\left(\frac{\Lambda_{\rm th}}{\overline{l}}\right)^5\sum_{n=1}^{\infty}\frac{1}{n^{3/2}}\prod_j\left[\frac{1}{n\beta\hbar\omega_j\lambda_j^2+2\alpha_j^2\overline{\alpha_j^2}}\right]^{1/2}\frac{\alpha_i}{n\beta\hbar\omega_i\lambda_i^2+2\alpha_i^2\overline{\alpha_i^2}}$$
$$\times\left[1+\frac{2n\beta m\omega_i^2[\eta_i^{(2)}-\eta_i^{(1)}]^2}{n\beta\hbar\omega_i\lambda_i^2+2\alpha_i^2\overline{\alpha_i^2}}\right]\exp\left(\sum_i\frac{-n\beta m\omega_i^2[\eta_i^{(2)}-\eta_i^{(1)}]^2}{n\beta\hbar\omega_i\lambda_i^2+2\alpha_i^2\overline{\alpha_i^2}}\right). \tag{A4}$$

[1] M. H. Anderson, J. R. Ensher, M. R. Matthews, C. E. Wieman, and E. A. Cornell, Science **269**, 198 (1995).
[2] C. C. Bradley, C. A. Sackett, J. J. Tollett, and R. G. Hulet, Phys. Rev. Lett. **75**, 1687 (1995); C. C. Bradley, C. A. Sackett, and R. G. Hulet, *ibid.* **78**, 985 (1997).
[3] K. B. Davis, M. O. Mewes, M. R. Andrews, N. J. van Druten, D. S. Durfee, D. M. Kurn, and W. Ketterle, Phys. Rev. Lett. **75**, 3969 (1995).
[4] N. P. Proukakis and K. Burnett, J. Res. Natl. Inst. Stand. Technol. **101**, 457 (1996).
[5] L. P. Kadanoff and G. Baym, *Quantum Statistical Mechanics* (Addison-Wesley, New York, 1962).
[6] E. Zaremba, A. Griffin, and T. Nikuni, Phys. Rev. A **57**, 4695 (1998).
[7] V. Shenoy and T.-L. Ho, Phys. Rev. Lett. **80**, 3895 (1998).
[8] G. M. Kavoulakis, C. J. Pethick, and H. Smith, Phys. Rev. A **57**, 2938 (1998).
[9] D. M. Stamper-Kurn, H.-J. Miesner, S. Inouye, M. R. Andrews, and W. Ketterle, Phys. Rev. Lett. **81**, 500 (1998).
[10] D. S. Jin, M. R. Matthews, J. R. Ensher, C. E. Wieman, and E. A. Cornell, Phys. Rev. Lett. **78**, 764 (1997).
[11] S. Stringari, Phys. Rev. Lett. **77**, 2360 (1996).
[12] K. G. Singh and D. S. Rokhsar, Phys. Rev. Lett. **77**, 1667 (1996).
[13] M. Edwards, P. A. Ruprecht, K. Burnett, R. J. Dodd, and C. W. Clark, Phys. Rev. Lett. **77**, 1671 (1996).
[14] Y. Castin and R. Dum, Phys. Rev. Lett. **77**, 5315 (1996).
[15] V. M. Pérez-Garcia, H. Michinel, J. I. Cirac, M. Lewenstein, and P. Zoller, Phys. Rev. Lett. **77**, 5320 (1996).
[16] R. J. Dodd, M. Edwards, C. J. Williams, C. W. Clark, M. J. Holland, P. A. Ruprecht, and K. Burnett, Phys. Rev. A **54**, 661 (1996).
[17] J. Javanainen, Phys. Rev. A **54**, R3722 (1996).
[18] L. You, W. Hoston, and M. Lewenstein, Phys. Rev. A **55**, R1581 (1997).
[19] P. Ohberg, E. L. Surkov, I. Tittonen, S. Stenholm, M. Wilkens, and G. V. Shlyapnikov, Phys. Rev. A **56**, R3346 (1997).
[20] D. S. Jin, J. R. Ensher, M. R. Matthews, C. E. Wieman, and E. A. Cornell, Phys. Rev. Lett. **77**, 420 (1996).
[21] M.-O. Mewes, M. R. Anderson, N. J. van Druten, D. M. Kurn, D. S. Durfee, C. G. Townsend, and W. Ketterle, Phys. Rev. Lett. **77**, 988 (1996).
[22] D. A. W. Hutchinson, E. Zaremba, and A. Griffin, Phys. Rev. Lett. **78**, 1842 (1997).
[23] R. J. Dodd, M. Edwards, C. W. Clark, and K. Burnett, Phys. Rev. A **57**, R32 (1998).
[24] M. Bijlsma and H. T. C. Stoof, Phys. Rev. A **54**, 5085 (1996).
[25] D. A. W. Hutchinson, R. J. Dodd, and K. Burnett, Phys. Rev. Lett. **81**, 4036 (1998).
[26] H. T. C. Stoof, J. Low Temp. Phys. **114**, 11 (1999).
[27] T. R. Kirkpatrick and J. R. Dorfmann, J. Low Temp. Phys. **58**, 301 (1985).
[28] P. Nozières and D. Pines, *The Theory of Quantum Liquids* (Addison-Wesley, New York, 1989), Vol. 1.
[29] N. P. Proukakis, K. Burnett, and H. T. C. Stoof, Phys. Rev. A **57**, 1230 (1998).
[30] V. N. Popov, *Functional Integrals in Quantum Field Theory and Statistical Physics* (Reidel, Dordrecht, 1983).
[31] J. D. Jackson, *Classical Electrodynamics* (Wiley, New York, 1975).
[32] E. A. Cornell (private communication).
[33] D. A. W. Hutchinson (private communication).
[34] H. T. C. Stoof, J. Stat. Phys. **87**, 1353 (1997).
[35] M. Houbiers and H. T. C. Stoof, Phys. Rev. A **54**, 5055 (1996).
[36] C. A. Sacket, H. T. C. Stoof, and R. G. Hulet, Phys. Rev. Lett. **80**, 2031 (1998).
[37] A. Minguzzi and M. P. Tosi, J. Phys.: Condens. Matter **9**, 10211 (1997).
[38] G. M. Kavoulakis, C. J. Pethick, and H. Smith, Phys. Rev. Lett. **81**, 4036 (1998).
[39] D. Guéry-Odelin, F. Zambelli, J. Dalibard, and S. Stringari, e-print cond-mat/9904409.